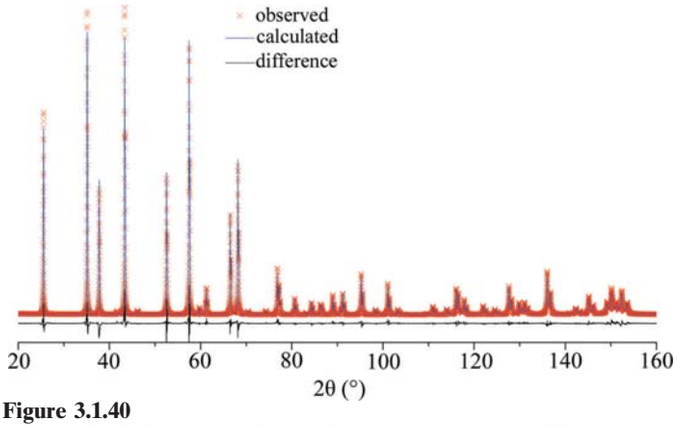

Figure 3.1.40
Fits of SRM 676a obtained from a Rietveld analysis using *GSAS* with the Thompson, Cox and Hastings formalism of the pseudo-Voigt PSF and the Finger model for asymmetry.

would have to be refined with a most basic calibration using an analysis of an SRM. The parameters to be refined for the emission spectrum include the positions and intensities of the $K\alpha_2$ profile, the satellite components and the tube tails. When addressing the $K\alpha_2$ profile, the relative positions and intensity ratios of the $K\alpha_{21}$ and $K\alpha_{22}$ Lorentzian profiles were constrained so as to preserve the overall shape as characterized by Hölzer *et al.* (1997). For the geometric profile, a single Soller-slit angle was refined, characterizing the degree of axial divergence and using the case-2 axial-divergence model applied to both the incident and diffracted beams. Other parameters of the geometric profile were fixed at known values. Additional parameters included a Lorentzian size-broadening term, background terms, and profile intensities and positions. A Gaussian microstrain term was included for analyses of SRM 1976b. Fig. 3.1.41 shows the quality of the fits obtained from an FPA analysis of SRM 660b. These fits present a substantial improvement over those using any of the analytical PSFs (Figs. 3.1.32 and 3.1.39). Furthermore, the GoF residual error term for an FPA profile analysis of a continuous scan of SRM 660b was 1.08, while the corresponding terms from analyses of the same data using the split pseudo-Voigt and split Pearson VII PSFs were 1.65 and 1.43, respectively (these three analyses were all from *TOPAS*). The FPA method can account for subtleties in the observed X-ray line profiles that analytical PSFs could never be expected to fit. In subsequent analyses of unknowns, it is not imprudent to fix parameters associated with the IPF; refining them, however, is typically not problematic with the FPA.

There were indications that the breadths of the profiles of the Cu $K\alpha$ emission spectrum as characterized by Hölzer *et al.* (1997) were in excess of those of our observations. This was investigated using the ultra-high-quality data. The FWHM ratios of the two pairs of Lorentzian profiles, the $K\alpha_{11}$ *versus* the $K\alpha_{12}$ and the $K\alpha_{21}$ *versus* the $K\alpha_{22}$, were constrained to those reported by Hölzer *et al.* (1997). The positions and intensities of the $K\alpha_2$ doublet were also refined, again with constraints applied to preserve the shape as per Hölzer *et al.* (1997). These refinements indicated that the breadths given by Hölzer *et al.* (1997) were significantly in excess of those that gave the best fit to the data. After an extensive investigation, this observation was confirmed to originate with the performance of the post-monochromator. Several graphite monochromator crystals were investigated using a beam diffracted from an Si single crystal (333 reflection) mounted in the specimen position. The graphite crystals that were manufactured within the last 15 years all gave identical results: after an alignment procedure to optimize the intensity of the $K\alpha_1$ line, they do clip the breadths of the profiles of the emission spectrum by approximately 20%. They also alter the position of diffraction lines by perhaps 0.01° in 2θ; therefore, the goniometer zero angles must be determined with the monochromator installed. We therefore used a reduced-breadth Hölzer emission spectrum in our FPA analysis. Note that these breadths vary with $\tan\theta$ because of angular dispersion, as does microstrain; therefore, only a microstrain-free specimen can be used for an analysis of the impact of a monochromator on the emission spectrum. We found that both SRMs 660c and 640e were suitable for this analysis.

The refinement strategy for the case-2 Soller-slit angle was also investigated with the ultra-high-quality data. Technically, the axial divergence of the incident beam, with the inclusion of the Soller slit, is less than that of the diffracted beam, which is limited by its extended beam-path length through the monochromator. Several strategies were investigated, some of which may have represented a more accurate physical model than that of a single divergence value applied to both beams, but none resulted in any improvement in the fit quality. Lastly, it was observed that the

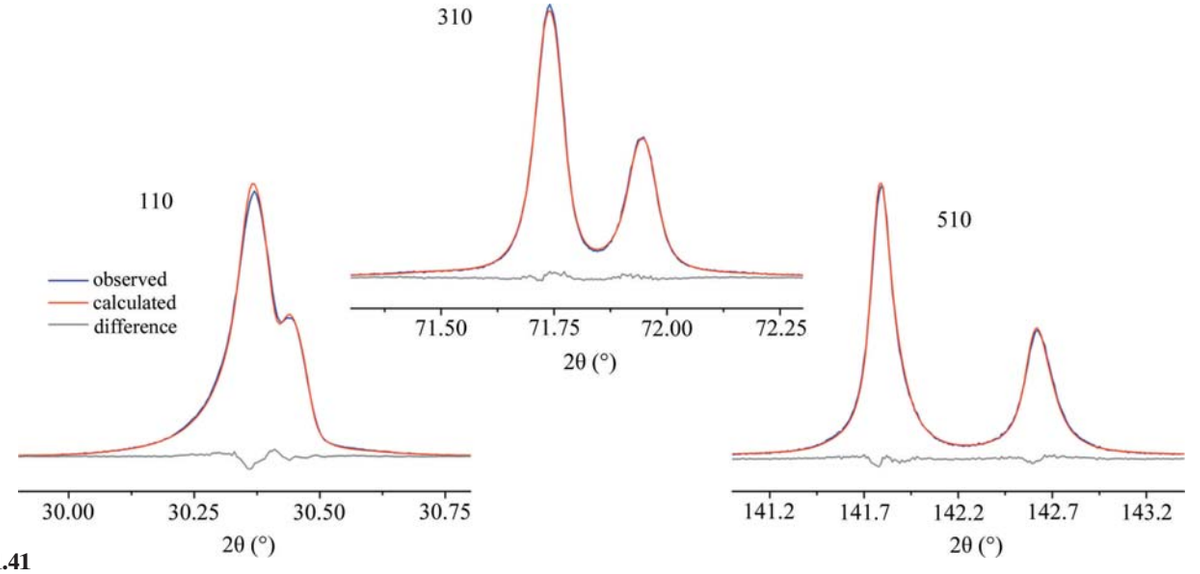

Figure 3.1.41
Fit quality realized with a fundamental-parameters-approach analysis of SRM 660b peak-scan data using *TOPAS*.